Journal of Integrative Neuroscience

J. Integr. Neurosci. **2026**; 25(8): 50217
https://doi.org/10.31083/JIN50217

Original Research

Shikonin Attenuates Neuroinflammation and Depression-Like Behaviors by Regulating Microglial Polarization Through Inhibiting cGAS-STING/NF-κB Signaling and Lipid Droplet Accumulation

Zi Chai[1,†], Wen-Ting Liu[2,†], Han-Yang Liu[1], Yuan-Yuan Su[1], Su-Yuan Ma[1], Hong-Tao Liang[1], Ya-Qin Li[1], Rui Liu[1,*]

[1]Department of Rehabilitation Medicine, Tangdu Hospital, The Fourth Military Medical University, 710038 Xi'an, Shaanxi, China
[2]Emergency Department, Tangdu Hospital, The Fourth Military Medical University, 710038 Xi'an, Shaanxi, China
*Correspondence: 289741154@qq.com (Rui Liu)
[†]These authors contributed equally.
Academic Editor: Domenico De Berardis
Submitted: 21 January 2026 Revised: 26 March 2026 Accepted: 8 April 2026 Published: 26 August 2026

Abstract

Background: Major depressive disorder is a disabling psychiatric illness with a growing global burden. Neuroinflammation, particularly microglial polarization, is increasingly recognized as a key pathogenic factor and is closely linked to lipid metabolic regulation. Shikonin, a bioactive naphthoquinone from *Lithospermum erythrorhizon*, exhibits anti-inflammatory and antioxidant properties, yet its antidepressant effects remain unclear. This study examined whether shikonin alleviates depressive-like behaviors by suppressing neuroinflammation. **Methods:** Mice were orally treated with shikonin for two weeks before the induction of learned helplessness (LH). A series of behavioral paradigms tail suspension test (TST), forced swim test (FST), sucrose preference test (SPT), and escapable shocks test (EST) was employed to evaluate depression-related behaviors. Following behavioral testing, inflammatory mediators, activation of the cyclic GMP-AMP synthase (cGAS)-stimulator of interferon genes (STING) pathway, microglial lipid droplet accumulation, autophagic status, and M1/M2 polarization markers were evaluated. *In vitro*, mouse microglial cell line BV2 (BV2) microglia were activated by lipopolysaccharide (LPS). A cell counting kit-8 (CCK-8) assay was conducted to screen non-cytotoxic shikonin concentrations, with subsequent *in vitro* verification of *in vivo* outcomes. The role of lipophagy in microglial polarization was further examined through pharmacological modulation of autophagy using chloroquine and rapamycin. **Results:** Shikonin markedly alleviated depression-like behaviors in LH mice, accompanied by decreased interleukin-6 (IL-6) and tumor necrosis factor-alpha (TNF-α) expression and inhibition of the cGAS-STING pathway. Mechanistically, shikonin suppressed M1 microglial polarization and lipid droplet accumulation in the hippocampus by restoring autophagic flux. Shikonin exerted anti-inflammatory effects *in vitro* by inhibiting cGAS-STING-dependent M1 polarization and restoring lipophagy in LPS-stimulated BV2 cells. **Conclusions:** Our findings show that shikonin suppresses cGAS-STING activation, shifts microglia away from the M1 phenotype, and promotes autophagy, thereby reducing lipid droplet accumulation and alleviating neuroinflammation and depressive-like symptoms.

Keywords: shikonin; depression; inflammation; lipid droplets; autophagy; learned helplessness model; cGAS-STING signaling pathway

1. Introduction

Depression is a highly prevalent mental disorder involving persistent affective disturbance, loss of pleasure, hopelessness, and multifaceted somatic and cognitive–behavioral impairments [1]. In severe cases, depression may result in suicide, underscoring its substantial public health impact [2]. In 2002, the World Health Organization ranked depression as the fourth largest contributor to the global burden of disease. The condition is further marked by frequent recurrence, long-lasting functional impairment, and an elevated risk of mortality [3]. Despite advances in pharmacological treatment, approximately 30% of patients exhibit resistance to antidepressant therapy, and nearly 70% fail to achieve complete remission with currently available interventions [4]. The pathogenesis of depression is multifactorial, involving neuroinflammatory processes, impaired neuroplasticity, dysregulation of the hypothalamic–pituitary–adrenal (HPA) axis, and disturbances in monoaminergic neurotransmission [5]. Increasing evidence indicates that inflammation is a critical pathogenic component. Proinflammatory cytokines have been shown to reduce 5-hydroxytryptamine (5-HT) levels, while interleukin-1β (IL-1β) and tumor necrosis factor-alpha (TNF-α) promote glutamate production, linking immune activation to neurotransmitter dysregulation [6,7]. Collectively, these findings emphasize the importance of elucidating the mechanisms by which inflammatory responses modulate depressive behaviors.

Microglia act as the primary immune responders in the central nervous system (CNS), playing key roles in neural maturation, tissue recovery, and maintenance of brain stability, while dynamically switching between inflammatory and anti-inflammatory activation states [8]. These polar-

ized states govern divergent functional programs and critically shape the magnitude and outcome of neuroinflammatory responses. Under conditions of chronic or excessive inflammation, pro-inflammatory cytokines both drive M1 polarization and amplify their own production while suppressing M2-associated programs. This feed-forward inflammatory loop damages both microglia and neurons and ultimately compromises neuroprotective functions. Consequently, the loss or reduction of M2 microglia impairs protective functions and underscores the therapeutic need to regulate the M1/M2 balance in neuroinflammation-associated disorders [9,10]. Emerging evidence indicates that autophagy and lipid metabolism are key regulators of microglial phenotype and function. Lipid droplets (LDs) are dynamic intracellular organelles, typically ranging from <1 to 100 μm in diameter, that serve as central sites for lipid storage and metabolic regulation. Structurally, LDs consist of a neutral lipid core rich in triacylglycerols (TGs) and cholesterol esters (CEs), enclosed by a phospholipid monolayer [11]. Lipophagy, a selective form of autophagy targeting LDs, is a major mechanism controlling LD turnover and intracellular lipid homeostasis. Notably, inflammatory stimuli, including lipopolysaccharide (LPS), elevated fatty acids, and aging, promote LD accumulation in both primary microglia and microglial cell lines [12]. Despite these observations, the mechanisms that dynamically regulate lipophagy in microglia under inflammatory conditions remain poorly understood.

The cyclic GMP-AMP synthase (cGAS)-stimulator of interferon genes(STING) and nuclear factor kappa-B (NF-κB) signaling pathways have attracted growing interest because of their involvement in neurotoxicity [13,14]. The cGAS-STING axis functions as a central regulator of inflammatory signaling. When cytosolic DNA originating from damaged nuclei, mitochondria, or invading pathogens is detected, cGAS generates the second messenger 2′3′-cGAMP, leading to activation of the adaptor protein STING [15,16]. STING activation recruits TANK Binding Kinase 1 (TBK1) and engages the inhibitor of kappa B kinase (IKK) complex, thereby stimulating the interferon regulatory factor (IRF3) and NF-κB pathways. This cascade drives the generation of type I interferons and proinflammatory cytokines, thereby potentiating innate immune responses. The cGAS-STING axis represents an emerging therapeutic target in immune-mediated, infectious, and malignant diseases due to its key role in immune regulation [17,18]. Notably, mitochondrial DNA–mediated activation of this pathway enhances microglia-driven neuroinflammation and has been linked to neurodegenerative disorders, including amyotrophic lateral sclerosis (ALS), Parkinson's disease (PD), and Alzheimer's disease (AD) [19]. In contrast, evidence linking the cGAS-STING axis to depression remains limited, and whether its modulation exerts antidepressant effects, as well as the underlying mechanisms, has yet to be elucidated.

Herbal and traditional Chinese medicines have shown therapeutic potential in CNS disorders, including PD, AD, and ischemic stroke. Shikonin, a principal naphthoquinone pigment isolated from the traditional herb *Lithospermum erythrorhizon*, exhibits anti-inflammatory, antioxidant, and antiapoptotic activities. Notably, shikonin can modulate BV2 microglial polarization and influence neuroinflammatory responses [20]. However, whether shikonin can alleviate depression-like behaviors and the mechanisms through which it influences neuroinflammation remain to be elucidated.

This work examined the potential antidepressant effects of shikonin and sought to clarify the mechanisms involved. Depressive-like behaviors were assessed using a learned helplessness (LH) mouse model, while neuroinflammatory processes were investigated in LPS-challenged BV2 microglial cells *in vitro*. Building on previous evidence that shikonin regulates microglial polarization and inflammatory signaling, the present findings demonstrate that shikonin attenuates depressive-like behaviors by inhibiting the cGAS-STING axis and reducing LD accumulation in microglia. Together, these results suggest a potential therapeutic strategy for depression and provide mechanistic insight into the involvement of microglial lipid metabolism and innate immune signaling in depressive pathology.

2. Materials and Methods

2.1 Materials

Shikonin (cat. no. S7576) and LPS (cat. no. L4391) were purchased from Sigma-Aldrich (St. Louis, MO, USA). Enzyme-linked immunosorbent assay (ELISA) kits for IL-6 (cat. no. JL20268) and TNF-α (cat. no. JL10484) were obtained from Jianglai Institute of Biotechnology (Shanghai, China). RIPA lysis buffer (cat. no. P0013B) and the CCK-8 assay kit (cat. no. C0038) were purchased from Beyotime Biotechnology (Shanghai, China). Protease (cat. no. P8340) and phosphatase (cat. no. P5726) inhibitor cocktails and the BCA protein assay kit (cat. no. 23225) were obtained from Sigma-Aldrich (St. Louis, MO, USA) and Thermo Scientific (MA, USA), respectively. Rabbit anti-inducible nitric oxide synthase (iNOS) antibody (1:1000, ab178945) was from Abcam (Cambridge, UK). The STING Pathway Antibody Sampler Kit (1:1000, #16029T) and antibodies against TNF-α (1:1000, #11948), arginase 1 (Arg1) (1:1000, #93668), NF-κB (1:1000, #8242), phospho-NF-κB (1:1000, #3033), IL-6 (1:1000, #12912), LC3B (1:1000, #12741), and sequestosome 1 (SQSTM1/p62) (1:10,000, #23214) were all from Cell Signaling Technology (Danvers, MA, USA). Rabbit anti-perilipin-2 antibody (1:10,000, 15294-1-AP) was from Proteintech Group (Wuhan, China). Rabbit antibodies against CD86 (1:100, GB13585) and CD206 (1:100, GB113497) were obtained from Servicebio Technology (Wuhan, China), and mouse anti-ionized calcium-binding adaptor molecule 1 (Iba-1) (1:100, A27316) and anti-β-

actin antibodies (1:10,000, AC026) were purchased from ABclonal Technology (Wuhan, China).

2.2 Animal Grouping

Male C57BL/6 mice (6–8 weeks) were maintained under controlled conditions with free access to food and water. Following a one-week acclimation, animals were randomly allocated into five groups: control, model, shikonin (1.2 mg/kg), shikonin (6 mg/kg), and shikonin (30 mg/kg).

2.3 Learned Helplessness Procedure and Drug Administration

Mice in the shikonin-treated groups were administered shikonin (1.2, 6, or 30 mg/kg) by daily intragastric gavage in 0.5% sodium carboxymethyl cellulose for 14 consecutive days. These doses were selected based on preliminary dose-ranging studies (0.6–60 mg/kg) that identified 1.2 mg/kg as the minimal effective dose showing behavioral improvement, 30 mg/kg as the maximal efficacious dose without observable toxicity (no weight loss or locomotor abnormalities), and 6 mg/kg as an intermediate dose to establish dose-dependency. This range aligns with previous reports demonstrating neuroprotective effects of shikonin at 5–25 mg/kg in rodent models of neuroinflammation and is well below the reported median lethal dose (LD50) (>100 mg/kg in mice). On day 12 of administration, mice in the model and shikonin groups underwent 180 inescapable foot shocks (0.3 mA, 6–10 seconds, intertrial interval 5–45 seconds). Animals in the control group were placed in the same apparatus without shock exposure. To eliminate residual olfactory cues, the chambers were disinfected with 75% ethanol between sessions [21]. Helpless behavior was assessed using the shuttle box test. Each mouse underwent a 3-minute adaptation period followed by 30 escapable shock trials (0.3 mA). Animals had 24 seconds to escape to the opposite chamber, at which point the shock terminated. Failure to escape within 24 seconds was recorded as an escape failure [22]. Escape failures and mean escape latency were recorded for each mouse. Following the LH assessment, depressive-like behaviors were further examined using the tail suspension test (TST), forced swim test (FST), and sucrose preference test (SPT). Mice were then euthanized by intraperitoneal injection of sodium pentobarbital (200 mg/kg body weight, 1% solution in sterile saline)(cat. no. P3761, Sigma-Aldrich, St. Louis, MO, USA), followed by cervical dislocation to ensure death. Hippocampal tissues were rapidly dissected on ice for subsequent experiments.

2.4 Behavioral Experiments

2.4.1 TST

Each mouse was suspended by the tail using adhesive tape in a three-walled chamber (30 × 15 × 15 cm), allowing free movement without obstruction. Behavioral activity was recorded on video for 6 min, and the duration of immobility, defined as a lack of active limb movements, was measured during the last 4 min of the session.

2.4.2 FST

Each mouse was tested individually in a clear cylindrical tank (14 cm diameter, 30 cm height) containing water (23–25 °C) to a depth of approximately half the cylinder height. Each session lasted 6 min and was video recorded. Immobility time, defined as the absence of active swimming except for movements required to remain afloat, was quantified during the final 4 min of the test.

2.4.3 SPT

Mice were habituated for 48 h to two drinking bottles containing tap water and 1% sucrose solution, with bottle positions alternated every 24 h. Following 24 h of water deprivation, the test was conducted for 12 h, during which both bottles were available and switched at 6 h. Fluid intake was determined by changes in bottle weight, and sucrose preference was calculated as the proportion of sucrose solution intake relative to overall liquid intake.

2.5 Cell Lines and Culture Conditions

The BV2 microglial cell line was obtained from the Cell Bank of the Chinese Academy of Sciences (Shanghai, China). All cell lines were authenticated by short tandem repeat (STR) profiling (GenePrint 10 System, Promega, Madison, WI, USA) within six months prior to the start of this study, and the results were compared with the American Type Culture Collection (ATCC) database to confirm the absence of cross-contamination. Additionally, all cells were routinely tested for mycoplasma contamination using a polymerase chain reaction (PCR)-based detection kit (cat. no. 30-1012K, ATCC, Manassas, VA, USA). The most recent test, conducted one week before the experiments, confirmed that all cell cultures were mycoplasma-negative.

2.6 Cell Viability Assay

BV2 microglial cells were seeded in 96-well plates (8×10^3 cells/well, 100 µL medium). After pre-culture, cells were exposed to shikonin (0, 0.25, 0.5, 1, 2.5, 5, 10, 20, or 50 µM) for 6, 12, or 24 h. Cells were exposed to the CCK-8 assay reagent (10 µL per well; Beyotime, China) and maintained for an additional 2 h. Absorbance values were then determined at 450 nm. Cell viability was normalized to the untreated control after correction for background signals [23].

2.7 Cell Culture and Treatments

BV2 microglia were maintained in high-glucose DMEM (cat. no. 11965092, Gibco, Thermo Fisher Scientific, Waltham, MA, USA) enriched with 10% fetal bovine serum (FBS) (cat. no. 10099141C, Gibco, Thermo Fisher Scientific) and 1% penicillin/streptomycin (cat. no. 15140122, Gibco, Thermo Fisher Scientific),

under standard culture conditions. Shikonin and 5,6-dimethylxanthenone-4-acetic acid (DMXAA) (cat. no. HY-10964, MedChemExpress, Monmouth Junction, NJ, USA) were dissolved in DMSO (cat. no. D2650, Sigma-Aldrich) and diluted in DMEM. Cells were assigned to six experimental groups: control, LPS, shikonin (2.5, 5, or 10 μM), and shikonin (10 μM) + DMXAA. Cells received shikonin pretreatment for 4 h before LPS challenge (1 μg/mL, 20 h), while the blockade group was pretreated with both shikonin (10 μM) and DMXAA (10 μg/mL) for 4 h prior to LPS stimulation.

For lipophagy analysis, BV2 cells were exposed to DMEM with 10% FBS and 1 μg/mL LPS for 18 h, followed by 50 μM chloroquine (CQ) (HY-17589A, MCE, Monmouth Junction, NJ, USA) for 6 h to block autophagosome–lysosome fusion. For autophagy induction, cells were pretreated with 10 nM rapamycin (RAPA) (HY-10219, MCE) for 30 min and then cultured for 24 h in medium containing 10% FBS, 1 μg/mL LPS, and 10 nM RAPA.

2.8 ELISA Assay

TNF-α and IL-6 levels in culture supernatants were determined by commercially available ELISA kits. Absorbance values at 450 nm were recorded with a microplate reader (Tecan Group Ltd., Männedorf, Zurich, Switzerland), and cytokine levels were quantified according to the standard curve.

2.9 Immunofluorescence Staining

BV2 microglia grown on poly-L-lysine–coated coverslips were exposed to LPS, shikonin before fixation with 4% paraformaldehyde (PFA) (cat. no. P6148, Sigma-Aldrich). Cells were permeabilized with PBS (cat. no. 10010023, Gibco, Thermo Fisher Scientific) containing 5% bovine serum albumin (BSA) (cat. no. A2153, Sigma-Aldrich) and 0.3% Triton X-100 (cat. no. T8787, Sigma-Aldrich), and sequentially incubated with primary antibodies (overnight at 4 °C) and secondary antibodies (2 h in the dark).

For brain tissue, mice were perfused, and brains were fixed in 4% PFA for 24 h at 4 °C. Cryosections (20 μm) were subjected to citric acid–based antigen retrieval (pH 6.0) and processed using the same immunostaining workflow as for BV2 cells. Sections were subsequently labeled with Cy3 for 10 min, counterstained with DAPI (cat. no. D3571, Invitrogen™, Thermo Fisher Scientific), mounted using an anti-fade medium, and examined by fluorescence microscopy (LG-FS80 Digital Slide Scanner, Wuhan Servicebio Technology Co., Ltd., Wuhan, China).

2.10 Western Blot (WB) Analysis

Following completion of behavioral assessments, bilateral hippocampi were rapidly isolated. Hippocampal samples and BV2 microglial cells were homogenized using RIPA lysis buffer containing protease and phosphatase inhibitor cocktails. Total protein concentrations were quantified with a BCA method. Equal protein amounts (20 μg) were resolved by SDS–PAGE and transferred onto 0.45 μm Polyvinylidene Fluoride (PVDF) membranes (cat. no. IPVH00010, MilliporeSigma, Burlington, MA, USA). After blocking with 5% non-fat milk in TBST, membranes were probed with primary antibodies targeting β-actin, iNOS, Arg1, IL-6, TNF-α, cGAS, STING, P-STING, TBK1, P-TBK1, IRF3, P-IRF3, NF-κB, P-NF-κB (1:1000), as well as PLIN2, LC3B, and p62 (1:10,000). HRP-conjugated goat anti-rabbit IgG (H+L) (1:5000, AS014, ABclonal Technology, Wuhan, China) and HRP-conjugated goat anti-mouse IgG (H+L) (1:5000, AS003, ABclonal Technology, Wuhan, China) were applied after three washes with TBST (cat. no. 28360, Thermo Fisher Scientific, 10 min each), and bands were detected by chemiluminescence and quantified using a ChemiScope 6200 system with Clinx software 6.3.1.0 (Clinx Science Instruments, Shanghai, China).

2.11 Statistical Analysis

Data are expressed as mean ± SEM. Normality was assessed using the Shapiro–Wilk test, and homogeneity of variances was evaluated using Levene's test. For multiple group comparisons, one-way analysis of variance (ANOVA) was performed, followed by Tukey's post-hoc test for pairwise comparisons. All statistical tests were two-tailed. Statistical analyses were conducted using GraphPad Prism 10 (GraphPad Software, San Diego, CA, USA), with statistical significance defined as $p < 0.05$.

3. Results

3.1 Shikonin Treatment Markedly Ameliorates Helpless and Depression-Like Behaviors in Mice Subjected to the LH Model

We evaluated the antidepressant-like effects of shikonin using the LH mouse model. The chemical structure of shikonin and the experimental timeline are presented in Fig. 1a and Fig. 1b, respectively. Exposure to inescapable electric shocks induced a robust LH phenotype, with increased escape failures and longer escape latencies in the shuttle box compared with controls ($p < 0.0001$). Oral shikonin treatment (30 mg/kg) significantly decreased escape failures and escape latency in LH mice ($p < 0.0001$; $p < 0.01$) (Fig. 1c,d). Consistent with the development of helplessness, shock-exposed mice also exhibited pronounced depression-like behaviors, including increased immobility in the FST and TST, as well as reduced sucrose preference, relative to controls ($p < 0.0001$ for all measures). Following two weeks of shikonin treatment (30 mg/kg), these behavioral deficits were significantly alleviated. Specifically, immobility time was reduced in both the FST and TST ($p < 0.001$; $p < 0.0001$), while sucrose preference was markedly elevated ($p < 0.01$) (Fig. 1e–g). Collectively, these results demonstrate that

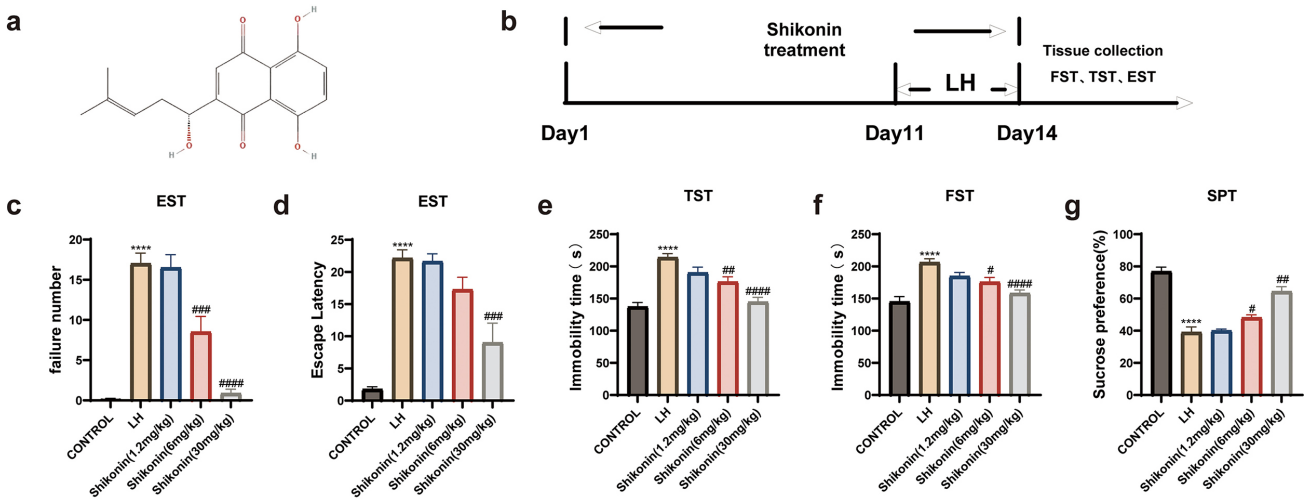

Fig. 1. Shikonin improves helpless-like and depressive-like behaviors in learned helplessness (LH) mouse. (a) Chemical structure of Shikonin. (b) Experimental design: mice received oral administration of Shikonin (1.2, 6, or 30 mg/kg) or vehicle for 14 consecutive days and were subjected to LH model stimuli on days 12–14. (c,d) The number of escape failures and the mean escape latency in the shuttle box were compared among groups using the escapable shock test (EST). (e–g) Shikonin (30 mg/kg) reversed the immobility time of LH mice in the forced swim test (FST) and tail suspension test (TST), and the decreased sucrose preference level in the sucrose preference test (SPT). n = 11 mice in each group. **** $p < 0.0001$ vs control group; # $p < 0.05$, ## $p < 0.01$, ### $p < 0.001$, #### $p < 0.0001$ vs LH group.

shikonin exerts a robust antidepressant-like effect in the LH model by reversing helplessness-associated escape deficits, behavioral despair, and anhedonia.

3.2 Shikonin Inhibits Neuroinflammation and Regulates Microglial Polarization State in the LH Mouse Model

WB analysis of hippocampal tissue was performed to assess inflammatory mediators and markers of microglial polarization, including iNOS and Arg1. LH exposure significantly increased IL-6, TNF-α, and iNOS concentrations while markedly decreasing Arg1 expression. These alterations were substantially reversed by high-dose shikonin treatment ($p < 0.01$; $p < 0.05$; $p < 0.0001$; $p < 0.0001$) (Fig. 2a,d–g). Consistent with these findings, ELISA analysis of frontal cortex tissue showed marked elevations of IL-6 and TNF-α in LH mice, which were significantly reduced by shikonin at 6 mg/kg and 30 mg/kg (all $p < 0.0001$) (Fig. 2b,c). Immunofluorescence analysis further demonstrated a substantial increase in CD86-positive cells in the hippocampus following LH exposure, indicative of enhanced microglial activation. Treatment with medium- and high-dose shikonin largely normalized the expression patterns of CD86 and CD206 (Fig. 2h).

3.3 Shikonin Regulates the cGAS-STING-NF-κB Axis in the LH Mouse Model

The cGAS-STING axis critically governs inflammatory activity, including cytokine regulation and cell fate decisions. Prior work has implicated aberrant activation of this pathway in neuroinflammation associated with multiple neurological disorders. For example, microglial cGAS activation has been shown to exacerbate neuronal inflammation and neurodegeneration in mouse models of PD [15]. To determine whether cGAS-STING signaling is involved in depression-related pathology, its activation status was examined in the LH mouse model. WB analysis revealed that LH exposure significantly increased hippocampal expression of cGAS and phosphorylated STING (p-STING) compared with control mice ($p < 0.05$; $p < 0.0001$) (Fig. 3a–c). To confirm pathway engagement, we examined downstream effectors TBK1, IRF3, and NF-κB (Fig. 3a). LH mice exhibited significantly increased ratios of phosphorylated to total protein for these signaling effectors ($p < 0.0001$; $p < 0.0001$; $p < 0.001$), consistent with activation of the cGAS-STING cascade. Notably, shikonin treatment (30 mg/kg) markedly suppressed this activation, as reflected by reduced cGAS expression and decreased phosphorylation of STING, TBK1, IRF3, and NF-κB ($p < 0.0001$; $p < 0.0001$; $p < 0.001$) (Fig. 3a–f).

3.4 Shikonin Can Restore the Impaired Lipophagy of Hippocampal Microglia in LH Mice and Reduce LD Accumulation

LD accumulation in hippocampal microglia was first assessed by co-immunostaining for the LD-associated protein perilipin 2 (PLIN2) and the microglial marker ionized calcium-binding adaptor molecule 1 (Iba-1). Immunofluorescence analysis revealed a marked increase in PLIN2-positive LDs within hippocampal microglia following exposure to the LH paradigm, indicating excessive

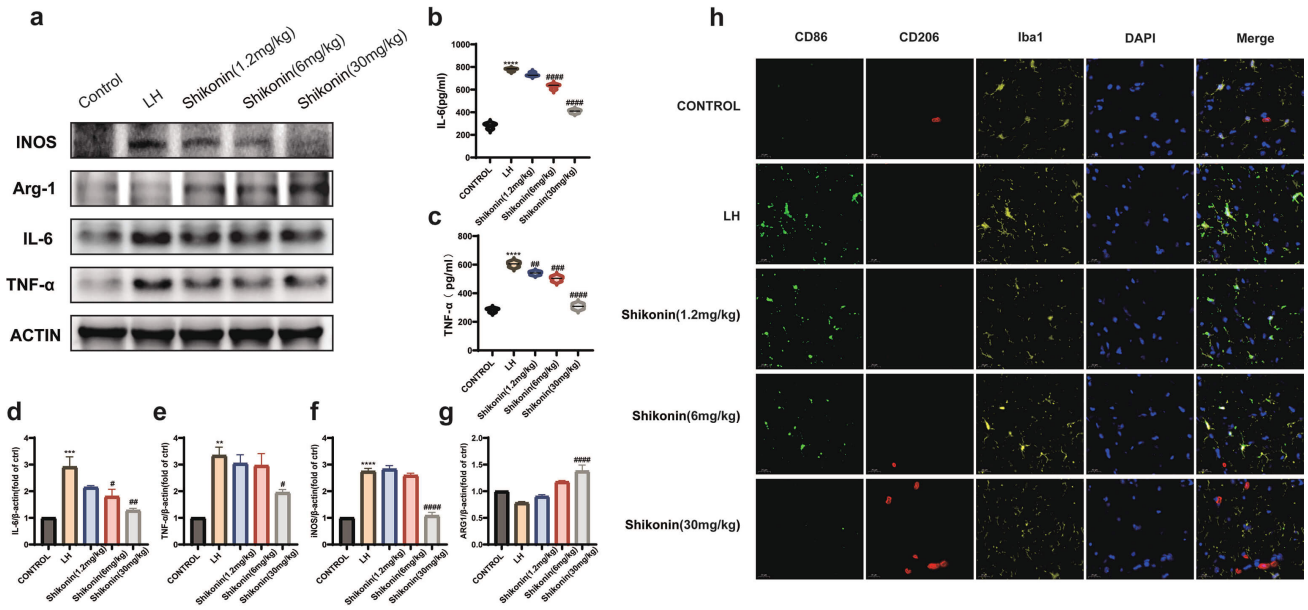

Fig. 2. Shikonin reduces neuroinflammation and restores microglial polarization in the hippocampus of LH mice. (a,d–g) Western blot analysis of pro-inflammatory cytokines (Interleukin-6, IL-6; Tumor necrosis factor-alpha, TNF-α) and microglial polarization markers, inducible nitric oxide synthase (iNOS) and arginase 1 (Arg1). (b,c) ELISA quantification of IL-6 and TNF-α levels in the frontal cortex. (h) Triple-label fluorescent immunocytochemistry provided representative images for each group: Blue (DAPI), Green (CD86), Red (CD206), Yellow (Iba-1). Scale bar = 20 μm. Data are presented as mean ± S.E.M. with significance denoted as, ** $p < 0.01$, *** $p < 0.001$, **** $p < 0.0001$ vs Control; # $p < 0.05$, ## $p < 0.01$, ### $p < 0.001$, #### $p < 0.0001$ vs LH group. n = 3.

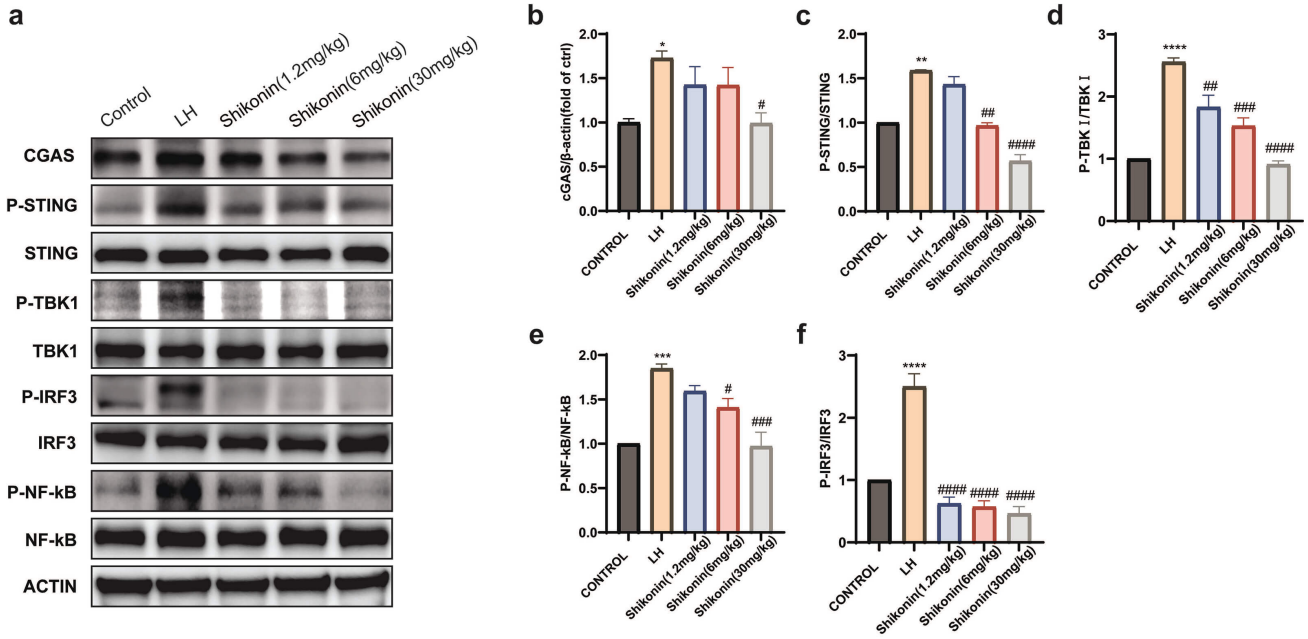

Fig. 3. The LH model stimulation activates the cyclic GMP-AMP synthase (cGAS)-stimulator of interferon genes (STING) pathway and its downstream factors in the mouse hippocampal tissue. (a–f) Western blot analysis of total cGAS, and total and phosphorylated forms of STING, TANK-binding kinase 1 (TBK1), interferon regulatory factor 3 (IRF3), and nuclear factor kappa-B (NF-κB) in hippocampal tissue. Quantitative analysis of the relative phosphorylation levels of STING (c), TBK1 (d), IRF3 (e), and NF-κB (f). Data are presented as mean ± S.E.M. * $p < 0.05$, ** $p < 0.01$, *** $p < 0.001$, **** $p < 0.0001$ vs the Control group; # $p < 0.05$, ## $p < 0.01$, ### $p < 0.001$, #### $p < 0.0001$ vs the LH group. n = 3.

lipid accumulation (Fig. 4a). Given that LDs are primarily degraded through autophagy-dependent lipophagy, microglial autophagic activity was subsequently examined. Hippocampal microglia from LH mice exhibited a pronounced reduction in LC3B puncta together with increased accumulation of SQSTM1/p62 puncta, suggesting impaired autophagic flux and defective lipophagic degradation of LDs (Fig. 4b,c). Notably, administration of shikonin (30 mg/kg) largely reversed these alterations. Shikonin treatment restored LC3B puncta formation (Fig. 4c,f), reduced SQSTM1/p62 accumulation (Fig. 4b,e), and significantly decreased the LD burden in hippocampal microglia, consistent with reactivation of lipophagy (Fig. 4a,d). Western blot analysis confirmed the immunofluorescence observations for PLIN2 and p62, showing increased protein levels in LH mice and their significant reduction following shikonin treatment (Fig. 4h–j). For LC3B, while immunofluorescence revealed restored LC3B puncta formation in shikonin-treated mice indicating renewed autophagosome biogenesis, Western blot analysis showed comparable LC3B levels between LH and shikonin groups, both remaining significantly lower than controls (Fig. 4g,j). This apparent discrepancy likely reflects the dynamic nature of autophagic flux: upon shikonin-induced reactivation of autophagy, increased autophagosome formation (detected as LC3B puncta by IF) coincides with rapid turnover and degradation of LC3B (detected as reduced steady-state protein levels by WB). The coordinated decrease in p62 accumulation—both in puncta number and total protein level—supports the conclusion that shikonin restores autophagic flux and lipophagic degradation of LDs.

3.5 Shikonin Modulates the cGAS-STING/NF-κB Signaling in LPS-Stimulated BV2 Cell Inflammation

The cytotoxicity of shikonin toward BV2 microglial cells was first assessed using the CCK-8 assay. Shikonin at concentrations ranging from 0.25 to 10 μM did not affect cell viability at 6, 12, or 24 h, whereas higher concentrations of 20 and 50 μM significantly reduced cell viability after 6, 12, or 24 h (Fig. 5a). On the basis of these findings, shikonin concentrations of 2.5, 5, and 10 μM were chosen for subsequent studies. To explore its regulatory mechanism, an *in vitro* inflammatory model was generated by LPS stimulation (1 μg/mL), which resulted in pronounced upregulation of cGAS and phosphorylated STING in BV2 cells ($p < 0.0001$; $p < 0.0001$) (Fig. 5b–d). LPS exposure robustly enhanced TBK1, IRF3, and NF-κB phosphorylation ($p < 0.0001$; $p < 0.0001$; $p < 0.001$) (Fig. 5b,e–g), whereas shikonin (10 μM) effectively reversed these effects by significantly suppressing their phosphorylation ($p < 0.001$; $p < 0.001$; $p < 0.01$) (Fig. 5b–g). These findings suggest that shikonin mitigates microglial inflammation through inhibition of the cGAS-STING/NF-κB signaling cascade.

3.6 Shikonin Suppresses LPS-Induced Neuroinflammation and BV2 Polarization via the cGAS-STING Axis

The involvement of shikonin in modulating LPS-evoked neuroinflammation and microglial polarization was further examined in BV2 cells. Cells were pre-exposed to shikonin (2.5, 5, or 10 μM) for 4 h prior to a 20 h LPS challenge (1 μg/mL). To determine the involvement of the cGAS-STING pathway, a parallel group was co-treated with shikonin (10 μM) and the STING agonist DMXAA (10 μg/mL). Shikonin dose-dependently attenuated TNF-α and IL-6 production triggered by LPS (Fig. 6a–c). Moreover, shikonin downregulated iNOS while upregulating Arg1, indicating attenuation of the neuroinflammatory response (Fig. 6a,d,e). Notably, these effects were abolished by co-treatment with DMXAA, indicating that the cGAS-STING axis is critical for the anti-neuroinflammatory actions of shikonin (Fig. 6a–e). Double immunofluorescence analysis demonstrated a marked increase in M1-polarized BV2 cells in the LPS model ($p < 0.0001$) (Fig. 6f,g). Pretreatment with shikonin (10 μM) significantly decreased the proportion of CD86-positive cells (M1 phenotype) while increasing CD206-positive cells (M2 phenotype) (all $p < 0.0001$) (Fig. 6f,h). Co-treatment with the cGAS-STING pathway activator DMXAA (10 μg/mL) reversed this effect ($p < 0.0001$) (Fig. 6f–h).

3.7 Shikonin Rescues Lipophagy Impairment and LD Accumulation in LPS-Stimulated Microglia

WB and immunofluorescence analyses showed that LPS (1 μg/mL) disrupted autophagic flux in BV2 microglia, accompanied by a pronounced increase in LD accumulation. To determine whether shikonin regulates microglial inflammatory status by modulating lipophagy and LD metabolism, BV2 cells were co-treated with shikonin during LPS exposure. Shikonin markedly reduced LPS-induced punctate accumulation of SQSTM1/p62 and PLIN2 and restored LC3B levels (Fig. 7a–g). In contrast, co-treatment with the autophagy inhibitor chloroquine (CQ) significantly attenuated the effects of shikonin, as evidenced by increased iNOS and PLIN2 expression compared with shikonin treatment alone (Fig. 7h,j–m). As a pharmacological positive control, the autophagy activator RAPA produced effects similar to shikonin treatment, reducing PLIN2 accumulation and inflammatory markers under LPS stimulation (Fig. 7i,n–q). It is important to emphasize that while RAPA demonstrates that enhanced autophagic flux correlates with reduced LD burden and inflammation, the definitive evidence establishing that shikonin acts through autophagy derives from the CQ inhibition experiments (Fig. 7h–m). The observation that CQ blocks shikonin's effects on PLIN2 and iNOS indicates that shikonin-mediated neuroprotection is strictly dependent on functional autophagy. Collectively, these results indicate that LD accumulation in BV2 cells under inflammatory stress is primarily driven by impaired lipophagy, and that

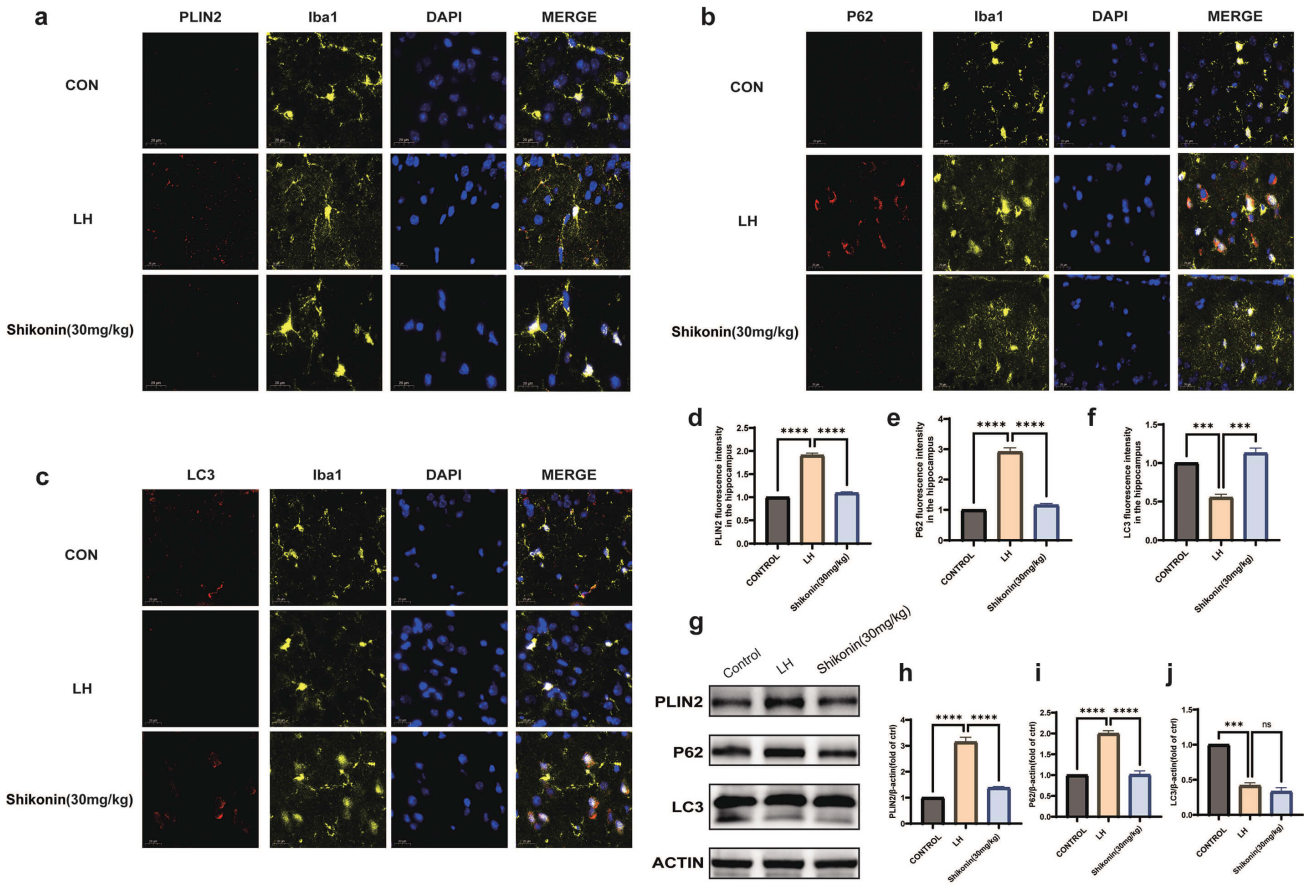

Fig. 4. Shikonin restores the impaired lipophagy of hippocampal microglia and reduces lipid droplet (LD) accumulation. (a–f) Double-label fluorescent immunocytochemistry provided representative images for each group. Scale bar = 20 μm. (g–j) Western blot analysis of key markers of autophagy (LC3B, p62) and lipid droplet protein markers (perilipin 2 (PLIN2)). Data are presented as mean ± S.E.M. with significance denoted as *** $p < 0.001$, **** $p < 0.0001$; ns $p > 0.05$. n = 3.

shikonin restores autophagic activity and lipid homeostasis through an autophagy-dependent mechanism.

4. Discussion

Depression is a multifaceted mental illness, with neuroinflammatory processes increasingly implicated as key drivers of its pathogenesis [24,25]. Microglia serve as key regulators of neuroinflammatory responses within the CNS. When polarized toward the pro-inflammatory M1 phenotype, microglia release excessive cytokines that amplify neuroinflammatory cascades. Accordingly, therapeutic strategies that suppress M1 activation while promoting the neuroprotective M2 phenotype have gained attention as potential antidepressant approaches [26,27]. Under pathological conditions, signals released from damaged cells preferentially drive microglial polarization toward the M1 phenotype at sites of injury, accompanied by a concomitant reduction in M2 microglia. This imbalance enhances cytokine production and establishes a self-reinforcing loop between neuronal injury and inflammation, further limiting M2-associated protective responses [28,29]. Prior work has shown that shikonin exerts neuroprotective and anti-inflammatory effects at concentrations of 1–12.5 μM. Based on these properties, the present study investigated whether shikonin exerts antidepressant effects by attenuating neuroinflammation and explored the underlying molecular mechanisms.

In vivo experiments demonstrated that shikonin significantly alleviated helplessness- and depression-like behaviors induced by the LH model. High-dose shikonin markedly reduced hippocampal IL-6, iNOS, and TNF-α expression while restoring Arg1 levels. Immunofluorescence analysis further confirmed that shikonin promoted microglial polarization toward an anti-inflammatory phenotype. Collectively, these findings indicate that shikonin exerts antidepressant effects by suppressing neuroinflammation through the modulation of microglial polarization.

cGAS-STING signaling represents a core pathway in innate immune defense. By sensing cytosolic self or mitochondrial DNA released under genotoxic stress, cGAS triggers downstream type I interferon production. Upon sensing cytosolic double-stranded DNA, cGAS generates 2′,3′-cGAMP, which triggers STING activation and its trafficking to the ER–Golgi intermediate compartment for TBK1

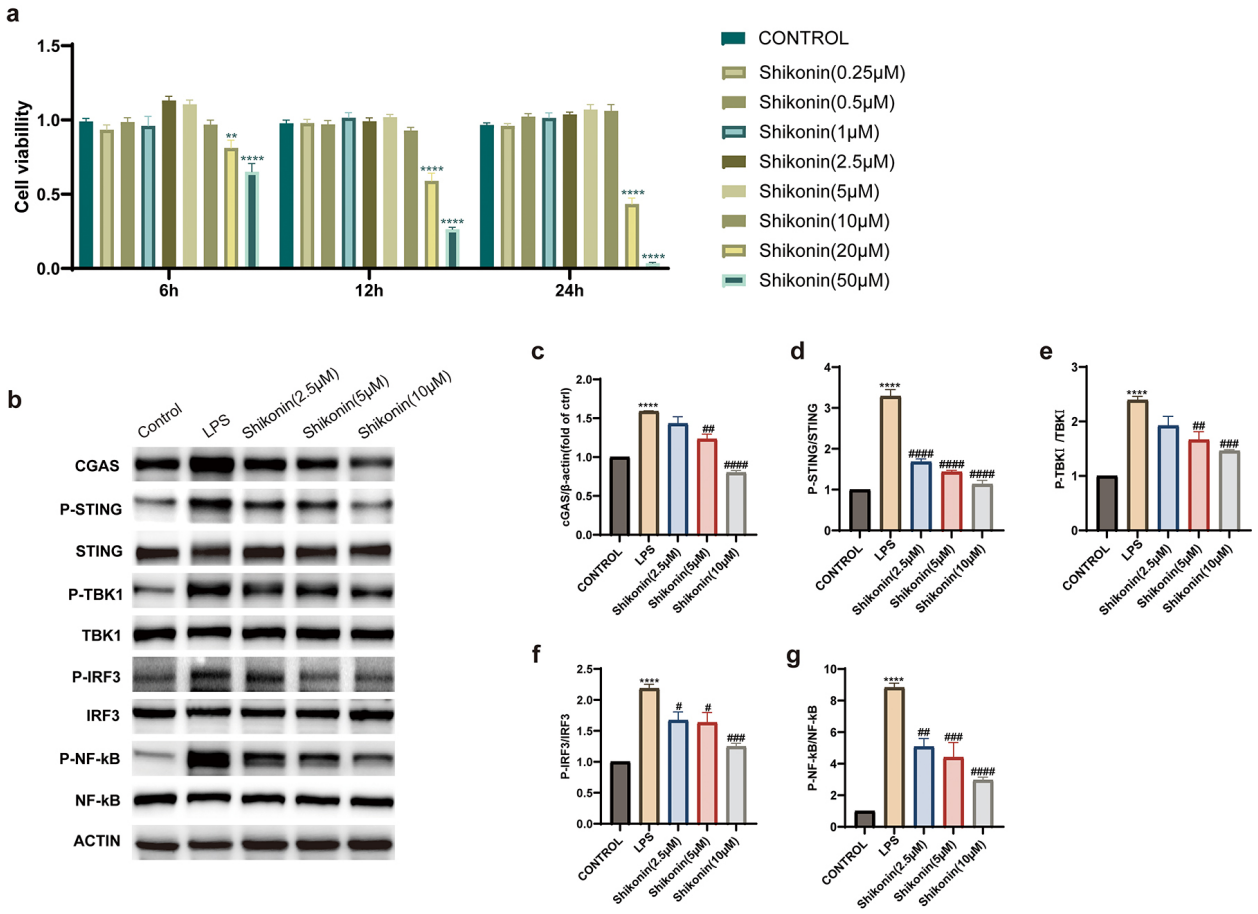

Fig. 5. Shikonin regulates the cGAS-STING/NF-κB signaling pathway in the lipopolysaccharide (LPS)-induced BV2 cell inflammation model. (a) BV2 cell viability with Shikonin treatment was assessed using the CCK-8 assay. (b–g) Western blotting was used to determine total and phosphorylated protein levels of cGAS, STING, TBK1, IRF3, and NF-κB. Quantitative analysis is shown for phosphorylation of STING (d), TBK1 (e), IRF3 (f), and NF-κB (g). Data are presented as mean ± S.E.M. ** $p < 0.01$, **** $p < 0.0001$ vs Control; # $p < 0.05$, ## $p < 0.01$, ### $p < 0.001$, #### $p < 0.0001$ vs LPS. n = 3.

and IKK engagement. This signaling complex induces IRF3 phosphorylation and NF-κB activation, with the latter further enhanced through STING-dependent IKK engagement and IκBα degradation. Activated IRF3 and NF-κB then translocate to the nucleus to induce the transcription of type I interferons and proinflammatory cytokines (TNF and IL-6). Beyond cytokine production, the cGAS-STING pathway regulates autophagy, cellular senescence, metabolism, and multiple forms of programmed cell death. Dysregulated activation of this pathway has been linked to neuroinflammatory processes in AD, PD, and Huntington's disease, whereas its involvement in depression remains largely unexplored [30]. Given the complex pathogenesis of depression and the limited efficacy of current treatments, identification of novel regulatory targets is urgently needed. Within this framework, the cGAS-STING axis is of particular interest due to its coordinated regulation of inflammation, autophagy, cellular metabolism, and programmed cell death. In this study, we detected dysregulation of the cGAS-STING/NF-κB pathway in brains from mice subjected to the LH model. Notably, high-dose shikonin markedly attenuated LH-induced activation of this pathway. Collectively, our findings suggest that shikonin exerts antidepressant-like effects through regulation of the cGAS-STING pathway, uncovering a novel link between innate immune signaling and depressive pathology. Analysis of our Western blot data reveals that shikonin treatment reduces both total cGAS protein expression and phosphorylated STING (p-STING) levels, alongside decreased phosphorylation of downstream TBK1, IRF3, and NF-κB. This dual effect suggests that shikonin may act at multiple levels—potentially suppressing cGAS transcription or promoting its degradation, while concurrently inhibiting STING phosphorylation/activation and its downstream recruitment of TBK1. However, Western blot analysis alone cannot distinguish whether shikonin directly inhibits enzymatic activity (e.g., blocking cGAS DNA sensing or STING palmitoylation) or acts through indirect transcriptional/epigenetic mechanisms.

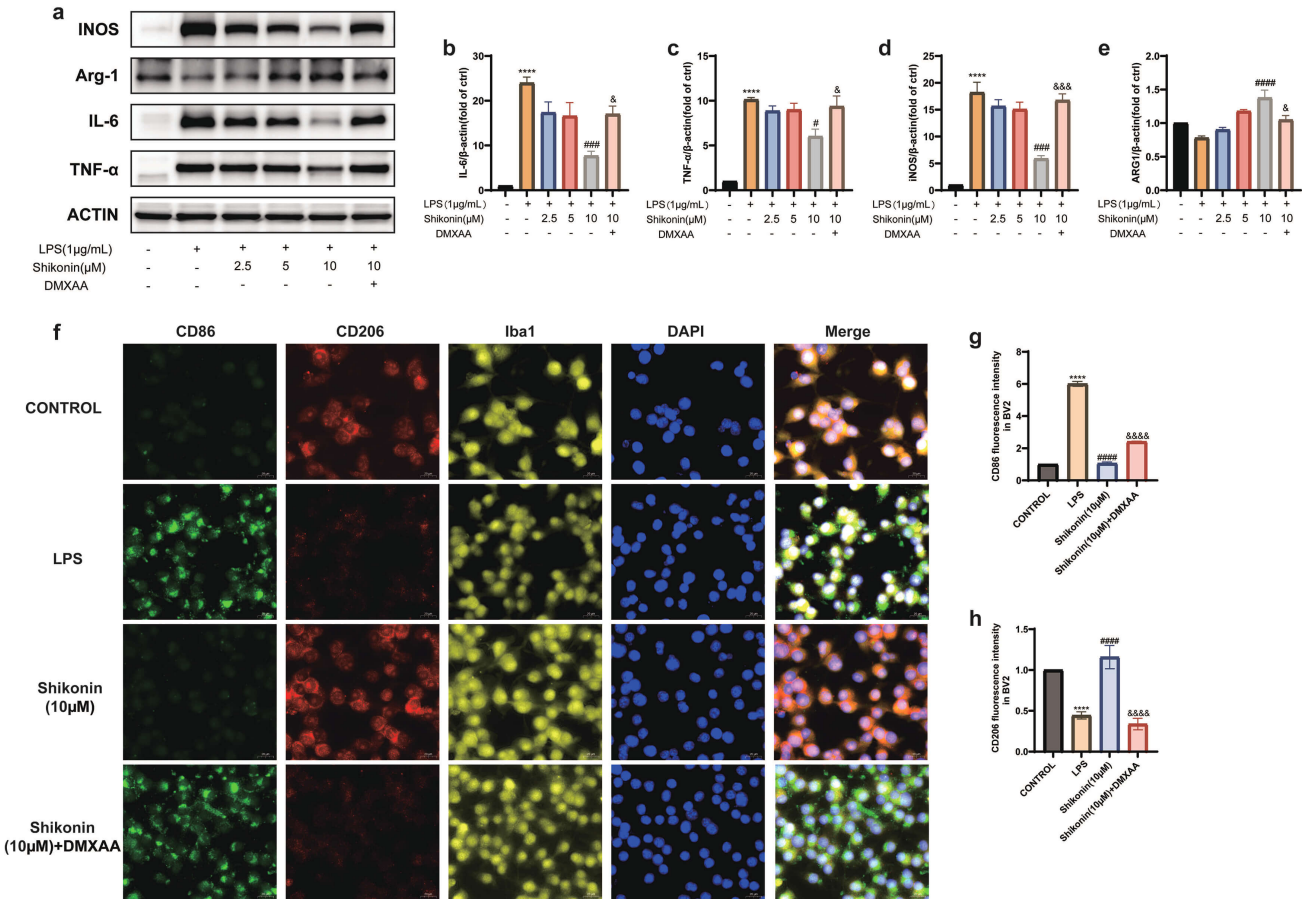

Fig. 6. Shikonin inhibits LPS-induced neuroinflammatory responses and influences the polarization of BV2 cells in LPS-stimulated BV2 cells via cGAS-STING pathway. (a–e) Shikonin significantly reduced LPS-induced pro-inflammatory protein expression in a dose-dependent manner, an effect reversed by the cGAS-STING agonist DMXAA. (f–h) Triple-label fluorescent immunocytochemistry provided representative images for each group: Blue (DAPI), Green (CD86), Red (CD206), Yellow (Iba-1). Scale bar = 20 μm. Data are presented as mean ± S.E.M. **** $p < 0.0001$ vs Control; # $p < 0.05$, ### $p < 0.001$, #### $p < 0.0001$ vs. LPS; & $p < 0.05$, &&& $p < 0.001$, &&&& $p < 0.0001$ vs Shikonin (10 μM). n = 3.

To precisely dissect the molecular node of intervention, we acknowledge that the present study employed the STING agonist DMXAA to demonstrate functional necessity of the pathway, but agonist reversal experiments cannot pinpoint whether shikonin acts upstream (cGAS), at the adaptor (STING), or downstream (TBK1/IRF3). Future studies employing specific pharmacological inhibitors—such as STING inhibitors (e.g., H-151, C-176), TBK1 inhibitors (e.g., MRT67307), or IKK inhibitors—combined with molecular docking and co-immunoprecipitation assays, will be essential to clarify whether shikonin physically interacts with cGAS, STING, or downstream kinases, and to determine the exact mechanism underlying its inhibitory effects.

LDs are present in the brains of patients with AD and in aged individuals, with enrichment primarily in the ventricular ependymal area [31]. In both rodents and humans, hypothalamic LD distribution varies between normal and disease states, including metabolic disorders and type 2 diabetes mellitus, underscoring their metabolic significance in the brain [32]. Microglia, the resident immune cells of the CNS, undergo functional alterations with aging [33]. In aged mice and humans, hippocampal microglia exhibit pronounced LD accumulation, reduced phagocytic capacity, and increased release of pro-inflammatory cytokines, collectively contributing to neurodegeneration. Previous research has identified lipolysis and lipophagy as the primary mechanisms for LD turnover. Through lipophagy, LDs are sequestered by autophagosomes and delivered to lysosomes for breakdown into free fatty acids [34,35]. Autophagy is a critical regulator of immune and inflammatory homeostasis, enabling the clearance of protein aggregates and damaged organelles. Disruption of autophagy is a pathological hallmark of neurodegeneration. Although recent studies have begun to address microglial autophagy, most have focused on AD and metabolic diseases, leaving its role in depression inadequately explored [36,37]. In the LH model of depression, prominent LD accumulation

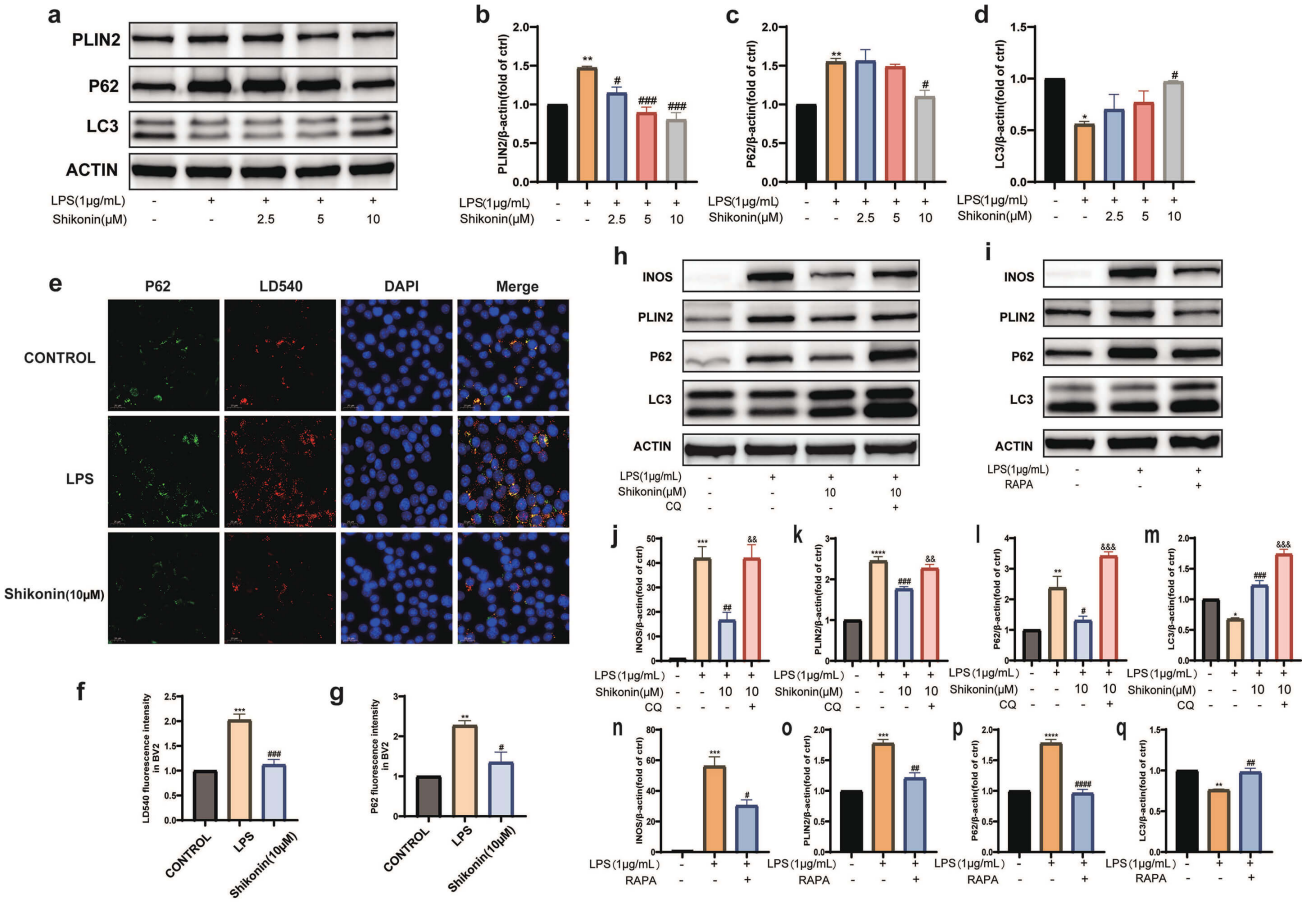

Fig. 7. Shikonin reversed impairment of lipophagy and accumulation of LDs in LPS-stimulated microglia. (a–d) Western blotting analysis of LC3B, p62 and PLIN2 expressions in BV2 cells co-treated with LPS and shikonin. (e–g) Representative micrographs of BV2 cells co-treated with LPS and shikonin. Lipophagy was visualized using p62 puncta, and LDs were visualized using LD540 puncta. The numbers of SQSTM1 puncta and LD540 puncta were quantified. Blue: DAPI, Green: p62, Red: LD540. (scale bar = 20 μm). (h–q) BV2 cells were exposed to an autophagy inhibitor (CQ) and an autophagy activator rapamycin (RAPA). Western blot analysis of LC3B, p62, PLIN2 and iNOS indicated that shikonin reversed inflammatory polarization in BV2 cells by enhancing lipophagy. Data are shown as mean ± S.E.M. * $p < 0.05$, ** $p < 0.01$, *** $p < 0.001$, **** $p < 0.0001$ vs Control group; # $p < 0.05$, ## $p < 0.01$, ### $p < 0.001$, #### $p < 0.0001$ vs LPS group; && $p < 0.01$, &&& $p < 0.001$ vs Shikonin (10 μM) group. n = 3.

and disrupted autophagic flux were observed in hippocampal microglia. Oral administration of shikonin restored autophagic activity, enhanced lipophagic degradation of LDs, and reduced their excessive accumulation within microglia. Notably, the temporal correspondence between changes in LD dynamics and modulation of the cGAS-STING signaling raises the possibility that shikonin regulates microglial lipid metabolism via a mechanism potentially involving the cGAS-STING axis.

To validate the *in vivo* findings and further elucidate the mechanism of action, an *in vitro* inflammatory model was established by stimulating BV2 microglial cells with LPS [38]. Consistent with the animal data, high-dose shikonin significantly attenuated LPS-driven proinflammatory cytokine release, restrained M1 polarization, and suppressed activation of the cGAS-STING/NF-κB pathway. Notably, pharmacological activation of cGAS-STING with DMXAA abrogated these protective effects, supporting a causal involvement of cGAS-STING/NF-κB signaling in the anti-neuroinflammatory activity of shikonin. In parallel, LPS stimulation impaired lipophagy, the selective autophagic degradation of LDs, leading to excessive LD accumulation in microglia. Shikonin treatment restored lipophagic flux and reduced LD aggregation, indicating that reestablishment of lipid homeostasis represents a key therapeutic mechanism. Moreover, pharmacological modulation of autophagy with CQ and RAPA altered microglial polarization, further implicating lipophagy as a central regulator of microglial inflammatory homeostasis. While the present study did not directly assess the effects of the STING agonist DMXAA on specific autophagy markers (PLIN2, LC3, and p62), our revised conceptual framework positions microglial polarization as the central integrative phenotype. In this model, shikonin at-

tenuates neuroinflammation by regulating microglial polarization through two coordinated mechanisms: inhibition of cGAS-STING/NF-κB signaling and restoration of lipophagy-dependent lipid droplet clearance. The functional evidence supports this cascade: DMXAA reversed shikonin-mediated suppression of M1 polarization, while chloroquine abolished shikonin's effects by blocking autophagy, indicating that the anti-inflammatory action of shikonin is autophagy-dependent. Although direct demonstration of DMXAA effects on PLIN2, LC3, and p62 would provide additional molecular granularity, the existing pharmacological data—combined with literature documenting that cGAS-STING activation impairs autophagic flux—support the proposed mechanism wherein cGAS-STING signaling regulates microglial function, at least in part, through modulation of lipophagy.

The present study has several limitations. Although our results suggest that shikonin influences cGAS-STING signaling, the specific molecular target underlying this regulation remains unclear. Future studies will incorporate target-prediction strategies, followed by experimental validation using approaches such as molecular docking and viral intervention, to clarify the direct mechanisms underlying its anti-neuroinflammatory activity. Moreover, although we inferred the relationship between cGAS-STING signaling and lipophagy based on functional data (DMXAA reversal of polarization and CQ inhibition of autophagy), direct experimental validation of how DMXAA modulates specific autophagy markers (PLIN2, LC3, and p62) was not performed. Future studies should incorporate Western blot analysis of these markers following DMXAA treatment to further delineate the precise molecular cascade linking STING activation to impaired lipophagy. Furthermore, LDs in the CNS act as a double-edged mechanism, providing early-stage protection but driving pathological progression when abnormally accumulated [39]. Existing studies report divergent effects of microglial LD synthesis and degradation on disease outcomes. In our study, enhancing lipophagy in hippocampal microglia of LH model mice reduced LD accumulation and attenuated neuroinflammation. In contrast, Arbaizar-Rovirosa et al. [40] reported that inhibiting microglial LD degradation conferred therapeutic benefits in mice following middle cerebral artery occlusion (MCAO) surgery. These apparently conflicting findings highlight the context-dependent nature of microglial LD dynamics, which may vary across disease types or across different stages within the same pathological process. To address this complexity, future investigations should employ multiple depression models, incorporate defined temporal sampling, and systematically characterize changes in microglial LDs to clarify how lipid metabolic reprogramming shapes neuroinflammatory responses. Additionally, the absence of a shikonin-alone treatment group (without LPS stimulation) in our *in vitro* experiments represents a limitation of the current study. Our experimental design focused on demonstrating shikonin's therapeutic potential in reversing established inflammatory states rather than assessing effects on homeostatic microglia. While CCK-8 assays confirmed no cytotoxicity on resting BV2 cell, formal assessment of shikonin effects on basal polarization markers and baseline autophagy in non-stimulated microglia remains to be performed. Future studies should include this control group to exclude potential confounding effects on resting microglial homeostasis.

From a translational perspective, shikonin exhibits pharmacokinetic properties favorable for CNS applications. As a lipophilic naphthoquinone (logP ~3.5), shikonin demonstrates oral bioavailability of 15–30% in rodents and documented blood–brain barrier permeability, with detectable levels in brain tissue following oral administration reported in previous neuroprotection studies. The effective dose used herein (30 mg/kg) is well below the acute LD50 (>100 mg/kg in mice), and chronic toxicity studies (4–12 weeks) have shown minimal hepatotoxicity or renal toxicity at doses ≤50 mg/kg/day. While shikonin has not completed phase III trials for depression, it has been used in traditional medicine for centuries, and modern clinical trials have evaluated its derivatives for inflammatory conditions and advanced malignancies (e.g., liposomal shikonin in phase I/II oncology trials). These considerations support the potential clinical translation of shikonin as a novel therapeutic for neuroinflammatory disorders, though further pharmacokinetic optimization and formal toxicology studies in depression models are warranted.

In summary, this study provided new insights and potential therapeutic avenues for treating depression. Our observations suggested that shikonin regulates the polarization state of microglia and alleviates neuroinflammation, thereby mitigating depressive-like behaviors, probably consequent to the inhibition of the cGAS-STING pathway. We also demonstrate that depressive mice exhibit impaired microglial lipophagy and concomitant accumulation of lipid droplets, and we provide evidence for a link between microglial polarization and lipid-droplet metabolism. Complementary *in vivo* and *in vitro* experiments show that shikonin restores microglial autophagic flux and thereby lowers pathological lipid-droplet accumulation. Nonetheless, additional research is essential to define precisely how shikonin modulates the cGAS-STING pathway and to clarify the mechanistic relationship between lipid metabolism and microglial polarization.

5. Conclusions

Collectively, our results indicate that shikonin alters the cGAS-STING/NF-κB signaling axis to drive BV2 microglia toward an M2 phenotype, producing measurable neuroprotective effects that alleviate depressive-like behaviors. Importantly, this study provides the first evidence that shikonin enhances microglial lipophagy in a depression model and reduces LD accumulation. Taken together, these

findings highlight the wide-ranging therapeutic promise of shikonin across neurological disorders and inflammatory diseases.

Availability of Data and Materials

The data supporting the findings of this study are available from the corresponding author upon reasonable request.

Author Contributions

Conceptualization, RL; methodology, ZC; software, ZC, WTL, YYS; validation, ZC, WTL, SYM; formal analysis, ZC, WTL, HTL, YQL; investigation, ZC, WTL, HYL; resources, RL; data curation, ZC, HYL; writing—original draft preparation, ZC; writing—review and editing, RL; visualization, ZC, YYS, SYM, HTL and YQL; supervision, RL; project administration, RL; funding acquisition, RL. All authors contributed to editorial changes in the manuscript. All authors read and approved the final manuscript. All authors have participated sufficiently in the work and agreed to be accountable for all aspects of the work.

Ethics Approval and Consent to Participate

The research was approved by the Laboratory Animal Welfare and Ethics Committee of the Fourth Military Medical University (approval No. 20220658). All procedures involving animals were performed in compliance with the NIH Guide for the Care and Use of Laboratory Animals (NIH Publication No. 80-23, revised 1996). Efforts were made to reduce the number of mice used and minimize their pain. The procedure strictly adhered to the approved guidelines of the Institutional Animal Care and Use Committee, emphasizing minimizing pain, ensuring swift death, and respecting animal life.

Acknowledgment

We gratefully acknowledge the assistance and instruction from scientific research supervisor of the Department of Rehabilitation Medicine of Tangdu Hospital.

Funding

The study was supported by the National Natural Science Foundation of China, No. 81771469 (to RL).

Conflicts of Interest

The authors declare no conflicts of interest.

References

[1] Won MS, Kim S, Yang YJ. Comparison of Health Status and Nutrient Intake between Depressed Women and Non-depressed Women: Based on the 2013 Korea National Health and Nutrition Examination Survey. Clinical Nutrition Research. 2016; 5: 112–125. https://doi.org/10.7762/cnr.2016.5.2.112

[2] Insel TR, Charney DS. Research on major depression: strategies and priorities. JAMA. 2003; 289: 3167–3168. https://doi.org/10.1001/jama.289.23.3167

[3] Yang G, Wang Y, Zeng Y, Gao GF, Liang X, Zhou M, et al. Rapid health transition in China, 1990-2010: findings from the Global Burden of Disease Study 2010. Lancet (London, England). 2013; 381: 1987–2015. https://doi.org/10.1016/S0140-6736(13)61097-1

[4] Kulkarni S, Dhir A, Akula KK. Potentials of curcumin as an antidepressant. TheScientificWorldJournal. 2009; 9: 1233–1241. https://doi.org/10.1100/tsw.2009.137

[5] Chevalier G, Siopi E, Guenin-Macé L, Pascal M, Laval T, Rifflet A, et al. Effect of gut microbiota on depressive-like behaviors in mice is mediated by the endocannabinoid system. Nature Communications. 2020; 11: 6363. https://doi.org/10.1038/s41467-020-19931-2

[6] Hiles SA, Baker AL, de Malmanche T, Attia J. A meta-analysis of differences in IL-6 and IL-10 between people with and without depression: exploring the causes of heterogeneity. Brain, Behavior, and Immunity. 2012; 26: 1180–1188. https://doi.org/10.1016/j.bbi.2012.06.001

[7] Xu X, Piao HN, Aosai F, Zeng XY, Cheng JH, Cui YX, et al. Arctigenin protects against depression by inhibiting microglial activation and neuroinflammation via HMGB1/TLR4/NF-κB and TNF-α/TNFR1/NF-κB pathways. British Journal of Pharmacology. 2020; 177: 5224–5245. https://doi.org/10.1111/bph.15261

[8] Wang J, Zhang G, Yang Y, Zhang X, Shi K, Zhang X, et al. *Schisandra chinensis* Lignans Exert Antidepressant Effects by Promoting BV2 Microglia Polarization toward the M2 Phenotype through the Activation of the Cannabinoid Receptor Type-2-Signal Transducer and Activator of Transcription 6 Pathway. Journal of Agricultural and Food Chemistry. 2022; 70: 14157–14169. https://doi.org/10.1021/acs.jafc.2c04565

[9] van Olst L, Rodriguez-Mogeda C, Picon C, Kiljan S, James RE, Kamermans A, et al. Meningeal inflammation in multiple sclerosis induces phenotypic changes in cortical microglia that differentially associate with neurodegeneration. Acta Neuropathologica. 2021; 141: 881–899. https://doi.org/10.1007/s00401-021-02293-4

[10] Guo S, Wang H, Yin Y. Microglia Polarization From M1 to M2 in Neurodegenerative Diseases. Frontiers in Aging Neuroscience. 2022; 14: 815347. https://doi.org/10.3389/fnagi.2022.815347

[11] Fujimoto T, Parton RG. Not just fat: the structure and function of the lipid droplet. Cold Spring Harbor Perspectives in Biology. 2011; 3: a004838. https://doi.org/10.1101/cshperspect.a004838

[12] Claes C, Danhash EP, Hasselmann J, Chadarevian JP, Shabestari SK, England WE, et al. Plaque-associated human microglia accumulate lipid droplets in a chimeric model of Alzheimer's disease. Molecular Neurodegeneration. 2021; 16: 50. https://doi.org/10.1186/s13024-021-00473-0

[13] Bai J, Liu F. The cGAS-cGAMP-STING Pathway: A Molecular Link Between Immunity and Metabolism. Diabetes. 2019; 68: 1099–1108. https://doi.org/10.2337/dbi18-0052

[14] Hopfner KP, Hornung V. Molecular mechanisms and cellular functions of cGAS-STING signalling. Nature Reviews. Molecular Cell Biology. 2020; 21: 501–521. https://doi.org/10.1038/s41580-020-0244-x

[15] Fu R, Shi L. Cross-talk between neuroinflammation and α-synuclein aggregation: The central role of the cGAS-STING pathway in Parkinson's disease. Cellular Signalling. 2026; 141: 112390. https://doi.org/10.1016/j.cellsig.2026.112390

[16] Paul BD, Snyder SH, Bohr VA. Signaling by cGAS-STING in Neurodegeneration, Neuroinflammation, and Aging. Trends in Neurosciences. 2021; 44: 83–96. https://doi.org/10.1016/j.tins.2020.10.008

[17] Ablasser A, Chen ZJ. cGAS in action: Expanding roles in immunity and inflammation. Science (New York, N.Y.). 2019; 363: eaat8657. https://doi.org/10.1126/science.aat8657
[18] Chen Q, Sun L, Chen ZJ. Regulation and function of the cGAS-STING pathway of cytosolic DNA sensing. Nature Immunology. 2016; 17: 1142–1149. https://doi.org/10.1038/ni.3558
[19] Zhong S, Zhou Q, Yang J, Zhang Z, Zhang X, Liu J, et al. Relationship between the cGAS-STING and NF-κB pathways-role in neurotoxicity. Biomedicine & Pharmacotherapy = Biomedecine & Pharmacotherapie. 2024; 175: 116698. https://doi.org/10.1016/j.biopha.2024.116698
[20] Zhao Y, Wang D, Mu D, Qu L, Li R. Shikonin alleviates rotenone-induced Parkinson's disease neuroinflammation by targeting PKM2-mediated glycolytic MG-Hs production. Cell Communication and Signaling : CCS. 2025; 23: 537. https://doi.org/10.1186/s12964-025-02542-z
[21] Worthen RJ, Garzon Zighelboim SS, Torres Jaramillo CS, Beurel E. Anti-inflammatory IL-10 administration rescues depression-associated learning and memory deficits in mice. Journal of Neuroinflammation. 2020; 17: 246. https://doi.org/10.1186/s12974-020-01922-1
[22] Li D, Zheng J, Wang M, Feng L, Liu Y, Yang N, et al. Wuling powder prevents the depression-like behavior in learned helplessness mice model through improving the TSPO mediated-mitophagy. Journal of Ethnopharmacology. 2016; 186: 181–188. https://doi.org/10.1016/j.jep.2016.03.065
[23] Tang X, Yan T, Wang S, Liu Q, Yang Q, Zhang Y, et al. Treatment with β-sitosterol ameliorates the effects of cerebral ischemia/reperfusion injury by suppressing cholesterol overload, endoplasmic reticulum stress, and apoptosis. Neural Regeneration Research. 2024; 19: 642–649. https://doi.org/10.4103/1673-5374.380904
[24] Sarapultsev A, Gusev E, Chereshnev V, Komelkova M, Hu D. Neuroimmune Interactions in Stress and Depression: Exploring the Molecular and Cellular Mechanisms within the Neuroinflammation-depression Nexus. Current Medicinal Chemistry. 2024. https://doi.org/10.2174/0109298673320710240920055041 (online ahead of print)
[25] Li P, Wang T, Guo H, Liu Y, Zhao H, Ren T, et al. Pramipexole improves depression-like behavior in diabetes mellitus with depression rats by inhibiting NLRP3 inflammasome-mediated neuroinflammation and preventing impaired neuroplasticity. Journal of Affective Disorders. 2024; 356: 586–596. https://doi.org/10.1016/j.jad.2024.04.073
[26] Block ML, Hong JS. Microglia and inflammation-mediated neurodegeneration: multiple triggers with a common mechanism. Progress in Neurobiology. 2005; 76: 77–98. https://doi.org/10.1016/j.pneurobio.2005.06.004
[27] Shi C, Qi Z, Yang C, Luo S, Huang S, Luo Y. Shikonin ameliorates depressive- and anxiogenic-like behaviors in rats via the suppression of inflammation in the hippocampus. Neuroscience Letters. 2024; 837: 137893. https://doi.org/10.1016/j.neulet.2024.137893
[28] Rentsch P, Egan T, Kuriakose A, Stayte S, Vissel B. The ratio of M1 to M2 microglia in the striatum determines the severity of L-Dopa-induced dyskinesias. Journal of Neurochemistry. 2023; 167: 633–647. https://doi.org/10.1111/jnc.15993
[29] Deng S, Zhang Z, Liu L, Xu C, Zhang D, Dong L, et al. The E3 ligase c-Cbl modulates microglial phenotypes and contributes to Parkinson's disease pathology. Cell Death Discovery. 2025; 11: 184. https://doi.org/10.1038/s41420-025-02482-0
[30] Decout A, Katz JD, Venkatraman S, Ablasser A. The cGAS-STING pathway as a therapeutic target in inflammatory diseases. Nature Reviews. Immunology. 2021; 21: 548–569. https://doi.org/10.1038/s41577-021-00524-z
[31] Shimabukuro MK, Langhi LGP, Cordeiro I, Brito JM, Batista CMDC, Mattson MP, et al. Lipid-laden cells differentially distributed in the aging brain are functionally active and correspond to distinct phenotypes. Scientific Reports. 2016; 6: 23795. https://doi.org/10.1038/srep23795
[32] Maya-Monteiro CM, Corrêa-da-Silva F, Hofmann SS, Hesselink MKC, la Fleur SE, Yi CX. Lipid Droplets Accumulate in the Hypothalamus of Mice and Humans with and without Metabolic Diseases. Neuroendocrinology. 2021; 111: 263–272. https://doi.org/10.1159/000508735
[33] Leng F, Edison P. Neuroinflammation and microglial activation in Alzheimer disease: where do we go from here? Nature Reviews. Neurology. 2021; 17: 157–172. https://doi.org/10.1038/s41582-020-00435-y
[34] Singh R, Kaushik S, Wang Y, Xiang Y, Novak I, Komatsu M, et al. Autophagy regulates lipid metabolism. Nature. 2009; 458: 1131–1135. https://doi.org/10.1038/nature07976
[35] Liu K, Czaja MJ. Regulation of lipid stores and metabolism by lipophagy. Cell Death and Differentiation. 2013; 20: 3–11. https://doi.org/10.1038/cdd.2012.63
[36] Bourdenx M, Martín-Segura A, Scrivo A, Rodriguez-Navarro JA, Kaushik S, Tasset I, et al. Chaperone-mediated autophagy prevents collapse of the neuronal metastable proteome. Cell. 2021; 184: 2696–2714.e25. https://doi.org/10.1016/j.cell.2021.03.048
[37] Li Q, Zhao Y, Guo H, Li Q, Yan C, Li Y, et al. Impaired lipophagy induced-microglial lipid droplets accumulation contributes to the buildup of TREM1 in diabetes-associated cognitive impairment. Autophagy. 2023; 19: 2639–2656. https://doi.org/10.1080/15548627.2023.2213984
[38] Hoogland ICM, Houbolt C, van Westerloo DJ, van Gool WA, van de Beek D. Systemic inflammation and microglial activation: systematic review of animal experiments. Journal of Neuroinflammation. 2015; 12: 114. https://doi.org/10.1186/s12974-015-0332-6
[39] Zhu XL, Zhang HW, Peng WJ, Gao S, Yang ZL, Zhang JQ, et al. Autophagy impairment is involved in midazolam-induced lipid droplet accumulation and consequent phagocytosis decrease in BV2 cells. Biochemical and Biophysical Research Communications. 2023; 643: 147–156. https://doi.org/10.1016/j.bbrc.2022.12.067
[40] Arbaizar-Rovirosa M, Pedragosa J, Lozano JJ, Casal C, Pol A, Gallizioli M, et al. Aged lipid-laden microglia display impaired responses to stroke. EMBO Molecular Medicine. 2023; 15: e17175. https://doi.org/10.15252/emmm.202217175